

## Inverse and direct energy cascades in 3D MHD turbulence at low-Rm

Nathaniel T. Baker,<sup>1,2,3</sup> Alban Pothérat,<sup>1</sup> Laurent Davoust,<sup>3</sup> and François Debray<sup>2</sup><sup>1</sup>Coventry University, Applied Mathematics Research Centre, Coventry CV15FB, UK<sup>2</sup>LNCMI-EMFL-CNRS, UGA, INSA, UPS 25 Ave. des Martyrs, 38000 Grenoble, France<sup>3</sup>Grenoble-INP/CNRS/Univ. Grenoble-Alpes, SIMaP EPM, F-38000 Grenoble, France

(Dated: 11 August 2017)

This experimental study analyzes the relationship between the dimensionality of turbulence and the upscale or downscale nature of its energy transfers. We do so by forcing low- $Rm$  magnetohydrodynamic (MHD) turbulence in a confined channel, while precisely controlling its dimensionality by means of an externally applied magnetic field. We first identify a specific lengthscale  $\hat{l}_\perp^c$  that separates smaller three-dimensional structures from larger quasi-two-dimensional ones. We then show that an inverse energy cascade of horizontal kinetic energy along horizontal scales is always observable at large scales, but that it extends well into the region of 3D structures. At the same time, a direct energy cascade confined to the smallest and strongly 3D scales is observed. These dynamics therefore appear not to be simply determined by the dimensionality of individual scales, nor by the forcing scale, unlike in other studies. In fact, our findings suggest that the relationship between kinematics and dynamics is not universal and may strongly depend on the forcing and dissipating mechanisms at play.

PACS numbers: Valid PACS appear here

Keywords: Magnetohydrodynamic (MHD) turbulence, Turbulence dimensionality, Turbulence dynamics, Inverse energy cascade

Turbulence displays radically opposite dynamics, whether it is three-dimensional (3D) or two-dimensional (2D). In the former, kinetic energy follows a direct energy cascade from the forcing scale down to the small dissipative scales controlled by viscosity<sup>1</sup>, while the latter features an inverse energy cascade from the forcing scale up to large structures of the size of the system<sup>2</sup>. Nevertheless, it is still unclear how these seemingly irreconcilable dynamics relate to each other, whenever 2D and 3D turbulent structures coexist.

This question is all the more crucial when dealing with real-life wall-bounded flows, as speaking of two-dimensionality only makes sense with respect to the presence of boundaries, such as no-slip walls. Yet, solid boundaries necessarily introduce three-dimensionality both in boundary layers and in the bulk<sup>3,4</sup>. As a result, real flows (such as oceans or atmospheres) can only be quasi-2D rather than strictly 2D, and often combine 2D and 3D turbulent structures<sup>5</sup>. The key question that determines both transport and dissipative properties of such flows is then how much, and which kind of three-dimensionality is required for the inverse cascade to become direct. In other words: how do the energy transfers relate to the topological dimensionality of turbulence?

It is unclear whether this question has a universal answer. Celani *et al.*<sup>6</sup> showed that compressing one dimension could yield a hybrid configuration, in which the energy flux split into a direct cascade at small scales and an inverse cascade at large scales. Xia *et al.*<sup>7</sup> showed that forcing a three-dimensional and three-component flow in a thick fluid layer could still produce a large coherent vortex, indicative of an upscale energy flux. Campaigne

*et al.*<sup>8</sup> showed in the context of rotating quasi-2D turbulence, that horizontal kinetic energy flowed preferentially upscale, while vertical kinetic energy flowed downscale. Finally, Biferale *et al.*<sup>9</sup> showed that a subset of the non-linear interactions of any 3D flow was in fact capable of transferring kinetic energy upscale.

We investigate this matter within the context of statistically steady liquid metal low- $Rm$  magnetohydrodynamic (MHD) turbulence in a homogeneous magnetic field<sup>10–12</sup>. A significant advantage of this approach is that the level of three-dimensionality of MHD turbulence can be controlled simply by adjusting the external magnetic field<sup>13–16</sup>. In particular, Ref.<sup>17</sup> theorised that a critical lengthscale separates (larger) quasi-2D from (smaller) 3D turbulent structures. More specifically, the two-dimensionalization of a turbulent structure of width  $l_\perp$  by the Lorentz force can be interpreted as the result of a “pseudo-diffusion” of momentum in the direction of the magnetic field<sup>17</sup>. The time  $\tau_{2D}(l_\perp)$  required to diffuse the momentum of a turbulent structure of size  $l_\perp$  over the distance  $l_z$  in the direction of the magnetic field is given by  $\tau_{2D} = (\rho/\sigma B_0^2)(l_z/l_\perp)^2$ . The other competing process is inertia, whose main effect is to redistribute kinetic energy across turbulent structures, by means of energy transfers. It takes place over the eddy turnover time  $\tau_u(l_\perp) = l_\perp/u(l_\perp)$ , where  $u(l_\perp)$  is the velocity of the structure at hand. The scaling law for the range of action of the Lorentz force follows from the balance between both effects<sup>17</sup>:

$$l_z(l_\perp) = l_\perp \sqrt{N(l_\perp)}, \quad (1)$$

where  $N(l_\perp, u(l_\perp)) = \sigma B_0^2 l_\perp / \rho u(l_\perp)$  is a scale-dependent

interaction parameter. The dimensionality of a structure is then determined by the presence of no-slip walls perpendicular to the magnetic field and distant by  $h$  through the ratio  $l_z(l_\perp)/h$ <sup>18,19</sup>. Indeed,  $l_z(l_\perp)/h \leq 1$  implies that velocity gradients exist in the bulk, in other words, that the structure of size  $l_\perp$  is 3D. Conversely,  $l_z(l_\perp)/h \gg 1$  implies that the Lorentz force can diffuse the momentum of the structure of size  $l_\perp$  over a distance much greater than  $h$ . This process is however blocked by the no slip-walls. The structure of size  $l_\perp$  is thus quasi-2D. It follows that the critical lengthscale  $l_\perp^c$  separating quasi-2D and 3D structures, for which  $l_z(l_\perp^c)/h = 1$ , expresses as<sup>17</sup>

$$\frac{l_\perp^c}{h} \sim \left[ \frac{\sigma B_0^2 h}{\rho u(l_\perp^c)} \right]^{-1/3} = N(h, u(l_\perp^c))^{-1/3}. \quad (2)$$

Increasing the externally applied magnetic field therefore offers a convenient way to broaden the spectrum of larger quasi-2D structures.

The problem at hand was tackled experimentally using the Flowcube<sup>18,20–22</sup>, an experimental platform designed to drive turbulence electrically in a deep rectangular vessel (100 mm high and 150 mm wide) filled with Galinstan (density  $\rho = 6400 \text{ kg/m}^3$ , electric conductivity  $\sigma = 3.4 \times 10^6 \text{ S/m}$ , kinematic viscosity  $\nu = 4 \times 10^{-7} \text{ m}^2/\text{s}$ ), and placed in a large solenoidal magnet delivering a near-homogeneous magnetic field of up to 10 T. In a nutshell, turbulent motions are induced by forcing a DC electric current  $I_0$  through a square periodic array of electrodes spaced either by  $l_i = 5$  or 15 mm located along the bottom wall<sup>20</sup>, while simultaneously applying a vertical and static magnetic field  $B_0 \mathbf{e}_z$  (cf. Fig. 1). The injection array is centered with respect to the bottom plate, which prevents the side walls from influencing the flow. The momentum resulting from the electric forcing applied at the bottom of the vessel is diffused by the solenoidal component of the Lorentz force in the direction of the magnetic field. Two complementary measurement methods were used to diagnose the resulting flow. On the one hand, a fine Cartesian mesh of probes mounted flush to the top and bottom walls along strips aligned with the  $\mathbf{e}_x$  direction gave access to the electric potential distribution at these walls. In the limit of high Hartmann number ( $Ha = B_0 h \sqrt{\sigma/\rho\nu}$ ) and interaction parameter, the potential along these horizontal walls is a precise estimate for the stream-function right outside the Hartmann boundary layer developing along them<sup>23</sup>. It thus provides both velocity components in the same planes. On the other hand, two ultrasound transducers were used to respectively measure the  $u_x(x)$  and  $u_z(z)$  velocity profiles through the bulk. The dimensionality of the flow is controlled through the single parameter  $l_z(l_i)/h$ , where  $l_z(l_i)$  is the diffusion length associated to turbulent structures of the size of the injection scale based on  $l_i$  and the RMS of the turbulent fluctuations measured along the bottom wall  $u_{\text{bot}}$ . The Reynolds number  $Re = u_{\text{bot}} h/\nu$  ranged between 32000 and 67000<sup>20</sup> throughout, which guarantees that turbulence is fully developed.

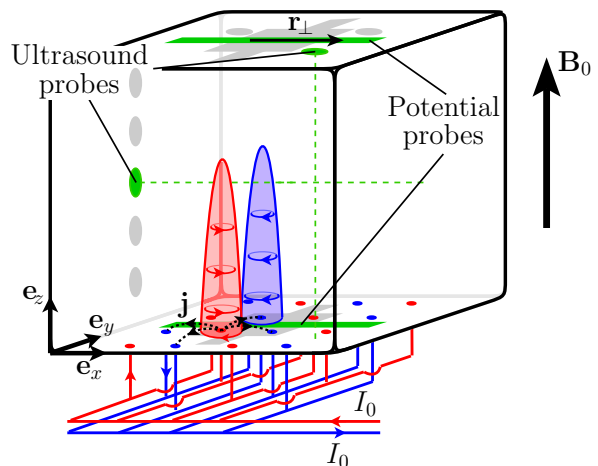


FIG. 1: Sketch of the Flowcube experiment. Results presented here were obtained by measuring the electric potential along strips of potential probes aligned with the  $\mathbf{e}_x$  direction located on the top and bottom plates, as well as a vertical and horizontal ultrasound probe.

Following Ref.<sup>24</sup>, we describe the structure of turbulence through the velocity increment  $\delta \mathbf{u} = \mathbf{u}(\mathbf{x} + \mathbf{r}) - \mathbf{u}(\mathbf{x})$ , computed from turbulent fluctuations. Due to the very low influence from the lateral walls<sup>20</sup>, the turbulence in Flowcube is considered homogeneous in the horizontal plane and axisymmetric. Hence,  $\mathbf{r}$  and  $\delta \mathbf{u}$  are respectively decomposed as  $\mathbf{r} = r_\perp \mathbf{e}_r + r_\parallel \mathbf{e}_z$ , and  $\delta \mathbf{u} = \delta \mathbf{u}_\perp + \delta \mathbf{u}_\parallel$ , with  $\delta \mathbf{u}_\parallel = (\delta \mathbf{u} \cdot \mathbf{e}_z) \mathbf{e}_z$  and  $\delta \mathbf{u}_\perp = \delta \mathbf{u} - \delta \mathbf{u}_\parallel$ . We focus on analyzing  $\delta \mathbf{u}_\perp(r_\perp \mathbf{e}_x)$  along both the top and bottom plates, where extensive data is obtained from electric potential measurements.

Let us start by analyzing the kinematics of the turbulence and attempt to discriminate 3D from quasi-2D structures. To do so, we adopt the signature function  $V$  as a scale-space alternative to the Fourier-space 3D energy spectrum<sup>25</sup>, which is expressed in 2D as<sup>26</sup>

$$V_\perp(r_\perp) = -\frac{r_\perp^2}{4} \frac{\partial}{\partial r_\perp} \frac{1}{r_\perp} \frac{\partial \langle \delta u_l^2 \rangle}{\partial r_\perp}. \quad (3)$$

Here,  $\delta u_l = [\mathbf{u}(\mathbf{x} + r_\perp \mathbf{e}_x) - \mathbf{u}(\mathbf{x})] \cdot \mathbf{e}_x$  is the longitudinal increment measured in the horizontal plane.

In axisymmetric turbulence, quasi-2D structures are invariant with respect to  $z$  outside the boundary layers. Their signature function must therefore be the same whether measured along the top or bottom walls. Conversely, any departure from a top/bottom mirror symmetry is an indication of a 3D structure. Fig. 2 shows the scale-wise distribution of horizontal turbulent kinetic energy across horizontal structures, along the top and bottom walls (referred to as  $V_\perp^{\text{top}}$  and  $V_\perp^{\text{bot}}$  respectively). As  $l_z(l_i)/h$  increases beyond one,  $V_\perp^{\text{top}}$  tends to match  $V_\perp^{\text{bot}}$ , both in shape and amplitude. Interestingly, the superposition of top and bottom energy distribu-

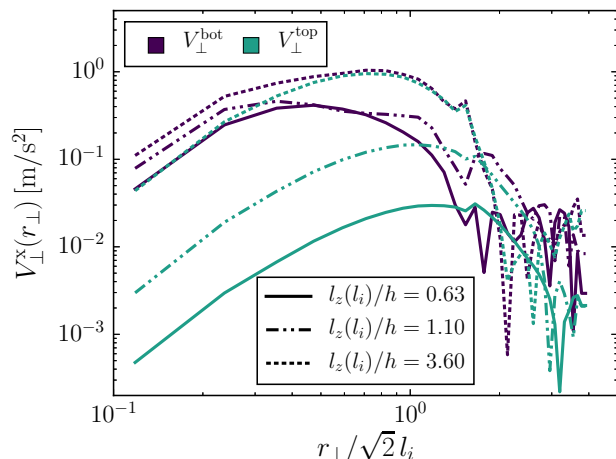


FIG. 2: Scale-wise perpendicular energy density along horizontal scales, measured by the signature functions  $V_{\perp}(r_{\perp})$  (normalization by  $\sqrt{2}$  comes from its very definition<sup>26</sup>). Comparing  $V_{\perp}^{\text{bot}}$  and  $V_{\perp}^{\text{top}}$  for increasing values of  $l_z(l_i)/h$  showcases the two-dimensionalization of smaller and smaller structures.

tions starts at large scales and works its way through smaller and smaller scales as  $l_z(l_i)/h$  increases. This behavior is in full agreement with Eq. (1), which states that it takes a higher field (i.e. a higher  $l_z(l_i)/h$ ) to make smaller structures quasi-2D. Note that a discrepancy remains between  $V_{\perp}^{\text{bot}}$  and  $V_{\perp}^{\text{top}}$  at small scales in the case  $l_z(l_i)/h = 3.60$ . The 3D to quasi-2D criterion  $l_z(l_i)/h = 1$  therefore provides a necessary rather than a sufficient condition for quasi-two dimensionality, and all the cases displayed in Fig. 2 possess three-dimensionality to some extent. Based on this observation, a lower bound for the smallest quasi-2D scale is obtained from the location of  $V_{\perp}^{\text{top}}(r_{\perp})$ 's maximum  $\hat{l}_{\perp}^c$ . Fig. 3 reports the variations of  $\hat{l}_{\perp}^c/l_i$  against the “true” interaction parameter  $N_t = N(h, u_{\perp}^c) \times (l_i/h)^2 = (l_z(l_i)/h)^2 (h/l_i)$ , which measures the ratio of diffusion by the Lorentz force to inertia<sup>27</sup>. Here,  $u_{\perp}^c = \sqrt{2 V_{\perp}^{\text{top}}(\hat{l}_{\perp}^c) \hat{l}_{\perp}^c}$  is an estimate for the velocity at the scale  $\hat{l}_{\perp}^c$ . All measurements collapse onto a single curve, of which two parts can be singled out. For  $N_t \lesssim 10^2$ ,  $\hat{l}_{\perp}^c/l_i \propto N_t^{-1/3}$ , which provides an experimental confirmation of Eq. (2). For  $N_t \gtrsim 10^2$ ,  $\hat{l}_{\perp}^c/l_i$  saturates towards a constant value of 0.62, as the critical scale becomes smaller than the smallest energy-containing scale.

Having identified quasi-2D and 3D regions of the scale space, we now seek regions where energy is transferred upscale and regions where it is transferred downscale. We first recall that the equation governing energy transfer in statistically steady MHD is the Kármán-Howarth equation, which reads, in the general inhomogeneous and

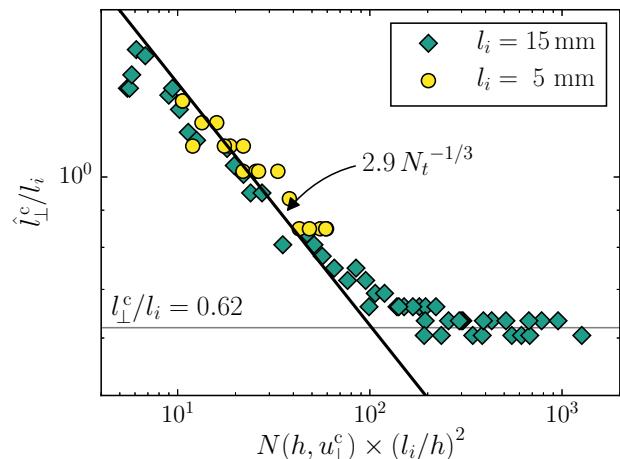


FIG. 3: 3D to quasi-2D critical lengthscale  $\hat{l}_{\perp}^c$ , as a function of the “true” interaction parameter  $N_t = N(h, u_{\perp}^c) \times (l_i/h)^2$ . The  $N_t^{-1/3}$  region indicates that the solenoidal component of the Lorentz force and inertia are competing with each other.

anisotropic case<sup>28</sup>

$$\Pi(\mathbf{r}) = \mathcal{P}(\mathbf{r}) + \mathcal{T}(\mathbf{r}) - \epsilon_J(\mathbf{r}) - \epsilon_{\nu}(\mathbf{r}). \quad (4)$$

In the above,  $\Pi(\mathbf{r}) = \nabla_{\mathbf{r}} \cdot \langle |\delta \mathbf{u}|^2 \delta \mathbf{u} \rangle$  quantifies the flux of turbulent kinetic energy in scale space,  $\mathcal{P}(\mathbf{r})$  is the rate of production of turbulent kinetic energy,  $\mathcal{T}(\mathbf{r})$  is the flux of turbulent kinetic energy in physical space (resulting from spatial inhomogeneities),  $\epsilon_J$  and  $\epsilon_{\nu}$  refer to energy dissipation via Joule damping and viscous friction respectively.  $\langle \cdot \rangle$  is an ensemble average, computed from time and spatial averages. In low- $Rm$  MHD, the energy transfers remain confined to the usual non-linear term found in hydrodynamics,

$$\Pi(\mathbf{r}) = \nabla_{\mathbf{r}} \cdot \langle |\delta \mathbf{u}|^2 \delta \mathbf{u} \rangle. \quad (5)$$

$\Pi(\mathbf{r})$  represents a local cumulative flux of kinetic energy exchanged between scales of size  $r$  and less, with those of size  $r$  and greater<sup>8</sup>:  $\Pi(r) > 0$  (*resp.*  $\Pi(r) < 0$ ) implies that, on average, energy flows towards scales larger (*resp.* smaller) than  $r$ , i.e. following an inverse (*resp.* direct) energy cascade. Invoking axisymmetry,  $\Pi(\mathbf{r})$  becomes a function of  $r_{\perp}$  and  $r_{\parallel}$  only, and (5) splits into four contributions:

$$\Pi_{\alpha}^{\beta} = \nabla_{\alpha} \cdot \langle |\delta \mathbf{u}_{\beta}|^2 \delta \mathbf{u}_{\alpha} \rangle, \quad (6)$$

where  $\alpha$  and  $\beta$  independently represent  $\perp$  or  $\parallel$ ,  $\nabla_{\perp} \cdot = (1/r_{\perp}) \partial_{r_{\perp}}(r_{\perp} \cdot)$ , and  $\nabla_{\parallel} \cdot = (\partial_{r_{\parallel}} \cdot) \cdot \mathbf{e}_z$ .  $\Pi_{\perp}^{\perp}$ ,  $\Pi_{\perp}^{\parallel}$ ,  $\Pi_{\parallel}^{\perp}$  and  $\Pi_{\parallel}^{\parallel}$  respectively represent the horizontal flux of horizontal energy, the horizontal flux of vertical energy, the vertical flux of horizontal energy and the vertical flux of vertical energy. None of  $\Pi_{\perp}^{\parallel}$ ,  $\Pi_{\parallel}^{\perp}$ , or  $\Pi_{\parallel}^{\parallel}$  can be precisely obtained from our measurements. Estimates for their

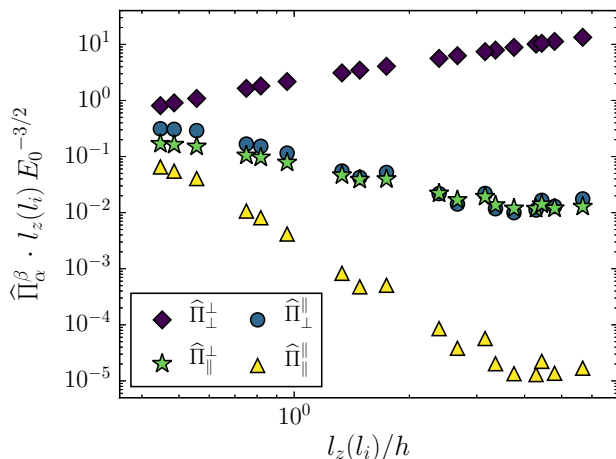


FIG. 4: Estimates for the different contributions to energy fluxes as a function of dimensionality, parametrized by  $l_z(l_i)/h$ . As  $l_z(l_i)/h$  extends beyond one, an increasing proportion of turbulent structures in the inertial range are quasi-2D.

orders of magnitude, defined as  $\hat{\Pi}_\alpha^\beta = \langle \mathbf{u}_\beta^2 \rangle \sqrt{\langle \mathbf{u}_\alpha^2 \rangle} / l_\alpha$ , may nevertheless be computed for all contributions.  $\langle \mathbf{u}_\perp^2 \rangle$  and  $\langle \mathbf{u}_\parallel^2 \rangle$  were computed as time and space-averages of one-dimensional velocity profiles obtained by ultrasound velocimetry. In addition, the lengthscales  $l_i$  and  $l_\parallel$  are respectively used to estimate  $\partial_{r_\perp}$  and  $\partial_{r_\parallel}$ .

Fig. 4 shows all  $\hat{\Pi}_\alpha^\beta$  against the dimensionality of turbulent structures of the size of the injection scale  $l_z(l_i)/h$ . The normalization involves  $l_z(l_i)$  and  $E_0 = [\langle \mathbf{u}_\perp^2 \rangle + \langle \mathbf{u}_\parallel^2 \rangle] / 2$  to account for varying energy levels injected from case to case. The only contribution to the energy transfers that strengthens, as the flow becomes quasi-2D is  $\hat{\Pi}_\perp^\perp$ . This reflects that in quasi-2D channel flows, (i) the vertical velocity component becomes very small compared to the horizontal one<sup>20,29</sup>, and (ii) velocity gradients along the magnetic field vanish. Consequently, any contribution to  $\Pi$  involving  $\delta \mathbf{u}_\parallel$  and/or  $\partial_{r_\parallel}$  must dwindle with  $l_z(l_i)/h$ . In the quasi-2D limit,  $\Pi_\perp^\perp \rightarrow \Pi$  as  $l_z(l_i)/h \rightarrow \infty$ . In any case, since  $\Pi_\perp^\perp$  remains greater than the sum of all other contributions, whether the flow is 3D or not,  $\Pi_\perp^\perp$  is representative of the total energy transfer  $\Pi$ .

Fig. 5 displays the horizontal transfer of horizontal kinetic energy between horizontal scales  $\Pi_\perp^\pm(r_\perp)$ , computed along the top and bottom Hartmann walls (referred to as  $\Pi_\perp^{\text{top}}$  and  $\Pi_\perp^{\text{bot}}$  respectively). The convergence level of these high order statistics is better than 1%<sup>20</sup>. The bulk of the transfers occur in the ranges  $0.5 \leq r_\perp/l_i \leq 1.5$  and  $r_\perp/l_i \geq 2$ . In both regions,  $\Pi_\perp^{\text{bot}}(r_\perp)$  and  $\Pi_\perp^{\text{top}}(r_\perp)$  are positive, so the energy transfer is upscale regardless of the value of  $l_z(l_i)/h$ , *i.e.* regardless of whether the corresponding structures are 2D or 3D. In the latter region, spatial oscillations whose period coincide with

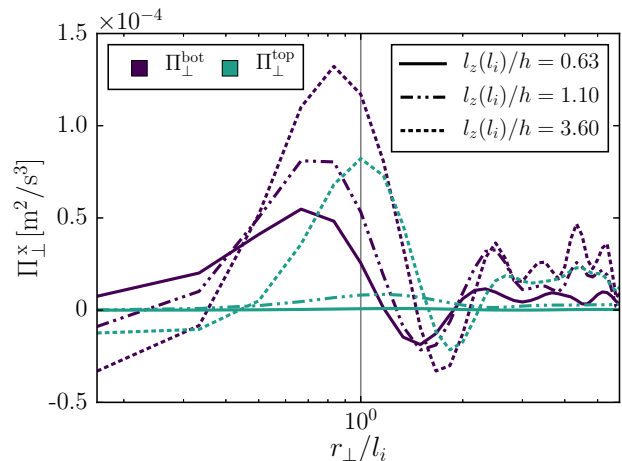


FIG. 5: Horizontal transfers of horizontal turbulent kinetic energy along the top and bottom walls:  $\Pi_\perp > 0$  implies a flux of kinetic energy towards larger scales. The vertical line locates the injection scale  $l_i$ .

the injection scale  $l_i$  exist, which may indicate an exchange of energy between scale and physical space, driven by the spatial inhomogeneities of the periodic forcing. Conversely, a small negative trough is visible for scales  $1.5 \leq r_\perp/l_i \leq 2$ . This range of structures is likely dominated by inertial instabilities resulting from the nearby injection scale, which leads to the non-random formation and breakup of vortex pairs<sup>22,30,31</sup>. At the upper end of spectrum, none of our numerous experiments displayed condensation into large turbulent structures, unlike studies using comparable forcing mechanisms<sup>32,33</sup>. It is likely that this difference comes from the presence of a stronger energy sink at large scales in our setup, due to the linear friction exerted by Hartmann layers on the quasi-2D structures<sup>11,17,34</sup>. Remarkably, two-dimensionality appears to promote a direct cascade at the lower end of the spectrum, at scales significantly smaller than the forcing scale ( $0 \leq r_\perp/l_i \leq 0.4$ ). Although this range never actually extends to the main forcing scale, it is all the closer to it as the flow is more quasi-2D. This may result from the increase of total kinetic energy associated to the two-dimensionalisation of the flow<sup>21</sup>.

While it is not surprising that quasi-2D structures always undergo an inverse cascade, it is remarkable that some 3D scales do and that the direct cascade only affects very strongly three-dimensional scales. These observations come in contrast with DNS of partly 2D and partly 3D non-MHD turbulence<sup>6</sup>, which show that the inverse cascade in non-MHD turbulence is confined to structures larger than the injection scale, while structures smaller than the injection scale experience a direct cascade. This main difference can probably be explained by the presence of Joule dissipation in our setup, which, according to Reddy & Verma<sup>35</sup>, tends to suppress the direct cascade. In any case, the present study shows that

energy transfers are not simply governed by the topological dimensionality of turbulence, but may also depend on the mechanisms promoting two-dimensionality and/or dissipation. The link between turbulence kinematics and dynamics is therefore very unlikely to be universal.

## ACKNOWLEDGMENTS

AP acknowledges support from the Royal Society under the Wolfson Research Merit Award Scheme (grant WM140032), the International Exchanges Scheme (Grant 140127), and from Grenoble-INP and Université Grenoble Alpes for the Invited professorship he has been granted. The laboratory SIMaP is part of the LabEx Tec 21 (Investissements d’Avenir - Grant Agreement No. ANR-11-LABX-0030).

- <sup>1</sup>L. Richardson, *Weather Prediction by Numerical Process* (Cambridge University, 1922).
- <sup>2</sup>R. Kraichnan, “Inertial ranges in two-dimensional turbulence,” *Phys. Fluids* **10**, 1417–1423 (1967).
- <sup>3</sup>J. Paret, D. Marteau, O. Paireau, and P. Tabeling, “Are flows electromagnetically forced in thin stratified layers two dimensional?” *Phys. Fluids* **9**, 3102–3104 (1997).
- <sup>4</sup>R. A. D. Akkermans, L. P. J. Kamp, H. J. H. Clercx, and G. H. F. Van Heijst, “Intrinsic three-dimensionality in electromagnetically driven shallow flows,” *Europhys. Lett.* **83**, 24001 (2008).
- <sup>5</sup>E. Lindborg, “Can the atmospheric kinetic energy spectrum be explained by two-dimensional turbulence?” *J. Fluid Mech.* **388**, 259–288 (1999).
- <sup>6</sup>A. Celani, S. Musacchio, and D. Vincenzi, “Turbulence in more than two and less than three dimensions,” *Phys. Rev. Lett.* **104**, 184506 (2010).
- <sup>7</sup>H. Xia, D. Byrne, G. Falkovich, and M. Shats, “Upscale energy transfer in thick turbulent fluid layers,” *Nature Phys.* **7**, 321–324 (2011).
- <sup>8</sup>A. Campagne, B. Gallet, F. Moisy, and P.-P. Cortet, “Direct and inverse energy cascades in a forced rotating turbulence experiment,” *Phys. Fluids* **26** (2014).
- <sup>9</sup>L. Biferale, S. Musacchio, and F. Toschi, “Inverse energy cascade in three-dimensional isotropic turbulence,” *Phys. Rev. Lett.* **108**, 164501 (2012).
- <sup>10</sup>P. Davidson, *An Introduction to Magnetohydrodynamics* (Cambridge University Press, 2001).
- <sup>11</sup>B. Knaepen and R. Moreau, “Magnetohydrodynamic turbulence at low magnetic reynold number,” *Ann. Rev. Fluid. Mech.* **40**, 25–45 (2008).
- <sup>12</sup>M. Verma, “Anisotropy in quasi-static magnetohydrodynamic turbulence,” *Rep. Prog. Phys.* **80**, 087001 (2017).
- <sup>13</sup>H. K. Moffatt, “On the suppression of turbulence by a uniform magnetic field,” *J. Fluid Mech.* **28**, 571–592 (1967).
- <sup>14</sup>A. Alemany, R. Moreau, P. Sulem, and U. Frisch, “Influence of an external magnetic field on homogeneous MHD turbulence,” *J. Méc.* **18**, 277–313 (1979).
- <sup>15</sup>S. Eckert, G. Gerbeth, W. Witke, and H. Langenbrunner, “Mhd turbulence measurements in a sodium channel flow exposed to a transverse magnetic field,” *Int. J. Heat and Fluid Flow* **22**, 358–364 (2001).
- <sup>16</sup>K. Messadek and R. Moreau, “An experimental investigation of MHD quasi-two-dimensional turbulent shear flows,” *J. Fluid Mech.* **456**, 137–159 (2002).
- <sup>17</sup>J. Sommeria and R. Moreau, “Why, how and when MHD turbulence becomes two-dimensional,” *J. Fluid Mech.* **118**, 507–518 (1982).
- <sup>18</sup>A. Pothérat and R. Klein, “Why, how and when MHD turbulence at low- $Rm$  becomes three-dimensional,” *J. Fluid Mech.* **761**, 168–205 (2014).
- <sup>19</sup>N. T. Baker, A. Pothérat, and L. Davoust, “Dimensionality, secondary flows and helicity in low- $Rm$  MHD vortices,” *J. Fluid Mech.* **779**, 325–250 (2015).
- <sup>20</sup>N. T. Baker, A. Pothérat, L. Davoust, F. Debray, and R. Klein, “Controlling the dimensionality of low- $Rm$  MHD turbulence experimentally,” *Exp. Fluids* **58**, 79 (2017).
- <sup>21</sup>A. Pothérat and R. Klein, “Do magnetic fields enhance turbulence at low magnetic Reynolds number?” *Phys. Rev. Fluids* **2**, 063702 (2017).
- <sup>22</sup>R. Klein and A. Pothérat, “Appearance of three-dimensionality in wall bounded MHD flows,” *Phys. Rev. Lett.* **104** (2010), 10.1103/PhysRevLett.104.034502.
- <sup>23</sup>A. Kljugin and A. Thess, “Direct measurement of the streamfunction in a quasi-two-dimensional liquid metal flow,” *Exp. Fluids* **25**, 298–304 (1998).
- <sup>24</sup>C. Lamriben, P.-P. Cortet, and F. Moisy, “Direct measurements of anisotropic energy transfers in a rotating turbulence experiment,” *Phys. Rev. Lett.* **107**, 024503 (2011).
- <sup>25</sup>P. Davidson and B. Pearson, “Identifying turbulent energy distributions in real, rather than Fourier, space,” *Phys. Rev. Lett.* **95**, 214501 (2005).
- <sup>26</sup>P. Davidson, *Turbulence: an introduction for scientists and engineers* (Oxford University Press, 2015).
- <sup>27</sup>B. Sreenivasan and T. Alboussière, “Experimental study of a vortex in a magnetic field,” *J. Fluid Mech.* **464**, 287–309 (2002).
- <sup>28</sup>R. Hill, “Exact second-order structure-function relationships,” *J. Fluid Mech.* **468**, 317–326 (2002).
- <sup>29</sup>A. Pothérat and K. Kornet, “The decay of wall-bounded MHD turbulence at low- $Rm$ ,” *J. Fluid Mech.* **783**, 605–636 (2015).
- <sup>30</sup>P. Tabeling, “Two-dimensional turbulence: a physicist approach,” *Phys. Rep.* **362**, 1–62 (2002).
- <sup>31</sup>A. Thess, “Instabilities in two-dimensional periodic flows part iii: Square eddy lattice,” *Phys. Fluids A* **4**, 1396–1407 (1992).
- <sup>32</sup>J. Paret and P. Tabeling, “Intermittency in the two-dimensional inverse cascade of energy: Experimental observations,” *Phys. Fluids* **10**, 3126–3136 (1998).
- <sup>33</sup>J. Sommeria, “Experimental study of the two-dimensional inverse energy cascade in a square box,” *J. Fluid Mech.* **170**, 139–168 (1986).
- <sup>34</sup>M. Chertkov, C. Connaughton, I. Kolokolov, and V. Lebedev, “Dynamics of energy condensation in two-dimensional turbulence,” *Phys. Rev. Lett.* **99**, 084501 (2007).
- <sup>35</sup>K. S. Reddy, R. Kumar, and M. K. Verma, “Anisotropic energy transfers in quasi-static magnetohydrodynamic turbulence,” *Phys. Plasmas* **21**, 102310 (2014).